Modelling soil erosion responses to climate change in three catchments of Great Britain

Rossano Ciampalini, J.A. Constantine, K.J. Walker-Springett, T.C. Hales, S.J. Ormerod, I.R. Hall

Modelling soil erosion responses to climate change in three catchments of Great Britain

R. Ciampalini[1,2], J.A. Constantine[3], K.J. Walker-Springett[1,4], T.C. Hales[1,5], S.J. Ormerod[4] and I.R. Hall[1]

[1] School of Earth and Ocean Sciences, Cardiff University, Cardiff CF10 3AT, UK

[2] LISAH, INRA, IRD, Montpellier SupAgro, Univ Montpellier, FR, 34060, Montpellier, FR

[3] Department of Geosciences, Williams College, Williamstown, Massachusetts 01267 USA

[4] Water Research Institute, School of Biosciences, Cardiff University, Cardiff CF10 3AT, UK

[5] Sustainable Places Research Institute, Cardiff University, Cardiff CF10 3AT, UK

Corresponding author: Rossano Ciampalini (rossano.ciampalini@gmail.com)

Abstract

Simulations of 21st century climate change for Great Britain predict increased seasonal precipitation that may lead to widespread soil loss by increasing surface runoff. Land use and different vegetation cover can respond differently to this scenario, mitigating or enhancing soil erosion. Here, by means of a sensitivity analysis of the PESERA soil erosion model, we test the potential for climate and vegetation to impact soil loss by surface-runoff to three differentiated British catchments. First, to understand general behaviours, we modelled soil erosion adopting regular increments for rainfall and temperature from the baseline values (1961-1990). Then, we tested future climate scenarios adopting projections from UKCP09 (UK Climate Projections) under the IPCC (Intergovernmental Panel on Climate Change) on a defined medium CO_2 emissions scenario, SRES-A1B (Nakicenovic et al., 2000), at the horizons 2010-39, 2040-69 and 2070-99. Our results indicate that the model reacts to the changes of the climatic parameters and the three catchments respond differently depending on their land use arrangement. Increases in rainfall produce a rise in soil erosion while higher temperatures tend to lower the process because of the mitigating action of the vegetation. Even under a significantly wetter climate, warmer air temperatures can limit soil erosion by enhancing primary productivity and in turn improving leaf interception, infiltration-capacity, and reducing soil erodibility. Consequently, for specific land uses, the increase in air temperature associated with climate change can modify the rainfall thresholds to generate soil loss, and soil erosion rates could decline by up to about 33% from 2070-2099. We deduce that enhanced primary productivity due to climate change can introduce a negative-feedback mechanism limiting soil loss by surface runoff as vegetation-induced impacts on soil hydrology and erodibility offset the effects of increased precipitation. The expansion of permanent vegetation cover could provide an adaptation strategy to reduce climate-driven soil loss.

Keywords

Soil erosion, Pesera model, sensitivity analysis, climate change, vegetation productivity

1. Introduction

Intensifying seasonal precipitation predicted to result from climate change (Kharin et al., 2007; O'Gorman and Schneider, 2009) will increase surface runoff and possibly rates of soil erosion (Boardman, 2013; Burt et al., 2016; Galy et al., 2015; Nearing et al., 2004; Lal, 2004;), thereby increasing economic costs associated with soil loss, which was as high £177m ($207m USD, 2019) in England and Wales alone (UK Environment Agency, 2019).

Surface runoff occurs as result of a number of natural mechanisms, including infiltration-excess overland flow, return flow, and direct precipitation onto saturated soil. These mechanisms may generate soil erosion by detaching and entraining soil particles over widespread areas (Hairsine and Rose, 1992; Whiting et al., 2001).

Vegetation can limit this process and may decrease the likelihood of surface runoff by reducing the intensity of rainfall through leaf interception as well as the moisture content of soil through transpiration (Zuazo et al., 2008). Nevertheless, its role in controlling surface runoff for assessing the potential climate-driven soil erosion by water remains uncertain (IPCC, 2019; Rogers et al. 2017).

Anthropogenic increases in atmospheric CO_2 concentrations may increase the water-use efficiency of plants by lowering transpiration rates, which could promote the generation of surface runoff by enhancing the moisture content of soil (Cramer et al., 2001; Gedney et al., 2006, Keenan et al., 2013). However, increased atmospheric CO_2 may also enhance plant productivity by acting as a fertilizer (Melillo et al., 1993), which could increase both plant water-usage and the infiltration capacity of soil through the addition of soil organic matter, thereby reducing the likelihood of surface runoff during precipitation events. Experimental results support predictions of increased plant productivity in response to elevated air temperatures and precipitation amounts (Piao et al., 2007; Walker et al., 2006), both of which are expected to increase in future climate scenarios (Boardman & Favis-Mortlock, 1993; Kharin et al., 2007; O'Gorman and Schneider, 2009).

The research of the climatic impact on soil erosion (Xiong et al., 2019) is typically based on erosion modelling techniques, of which extensive reviews are reported in Li & Fang (2016) and Pandey et al. (2016). Process-based models have been widely used in assessments of climate-driven impacts on soil erosion (e.g., Favis-Mortlock & Boardman, 1995; Luetzenburg et al., 2019; Mullan, 2012; Mullan et al., 2012; Nunes et al., 2013; Pastor et al., 2019, Routschek et al., 2014, 2015; Serpa et al., 2015), including impacts on vegetation and on agricultural practices in different climates (e.g., Garbrecht & Zhang, 2015; Nearing et al., 2005; O'Neal et al., 2005; Pruski and Nearing, 2002a; Scholz et al., 2008; Zhang et al., 2005, 2012). Despite of the large number of approaches existing for modelling erosion, process-based models are frequently uniquely suited for explicitly considering specific soil transport mechanisms and the impacts of climatic factors on soil hydrology (Guo et al., 2019).

In this research, we wanted to verify the hypothesis of how climate change and plant productivity affect soil erosion by surface runoff in a modelling approach. This was done by adopting a two-level procedure: 1) verifying the responses of soil erosion to changes in climate parameters (i.e. temperature and precipitation), 2) investigating the effects of future climate projections. For that, we opted to a process-based model implementable at spatial scales relevant to catchment-wide assessments of soil loss, in which catchments can be greater than 100 km^2 in size and be comprised of the full range of plant functional types. The Pan European Soil Erosion Risk Assessment (PESERA) model was specifically designed to accomplish such task (Kirkby et al., 2008).

PESERA calculates soil erosion via infiltration-excess overland flow by explicitly considering a range of physical processes controlling soil hydrology and has been successfully employed across many natural settings (e.g., Baggaley et al., 2010, De Vente et al., 2008; Esteves et al., 2012; Karamesouti et al., 2016; Licciardello et al., 2009; Meusburger et al., 2010; Pásztor et al., 2016; Tsara et al., 2005). PESERA only considers soil transfer by sheet wash and rilling during infiltration-excess overland flow, but both are widespread and pervasive mechanisms of soil transfer that can be simply and explicitly linked to land cover and climate, making it particularly useful for assessing the ability of vegetation to mitigate climate impacts on widespread soil loss. PESERA has also been used as base-platform to prepare similar models that implement procedures simulating other soil surface processes. These include PESERA-L (Borselli et al., 2011), which integrates sediment yield due to shallow mass movement, PESERA-DESMICE (Fleskens et al., 2016), which extends its functionalities to evaluate the agricultural financial viability of the measures to mitigate land degradation, and PESERA-PEAT (Li et al., 2016), where the model was modified to include blanket peat erosion processes. Some specific sensitivity analyses of PESERA also exist, such as that by Cheviron et al. (2010; 2011) who clarified the influence of the major model parameters, and Baggaley et al. (2017) who tested the effect of topography and soil erodibility characteristics.

We applied PESERA to three characteristic catchments comprised of the major land-cover types of Great Britain, similar to those in environments of temperate climates across the globe (Prentice et al., 1992). The Conwy (Wales), Ehen (England), and Dee (Scotland) catchments (Figure 1) are characterized by significant intra- and inter-catchment differences in topography, climate, soil and land use (Table 1), allowing us to describe the sensitivity of land-cover specific soil erosion to these variables. Further, the catchments have been recognized as important habitats for the endangered freshwater pearl mussel (Margaritifera margaritifera) (Cooksley et al., 2012; Joint Nature Conservation Committee, 2007), whose life cycles are negatively affected by fine-grained particulates derived from upland erosion (Geist & Auerswald, 2007).

Climatic responses to increased emissions of greenhouse gases are predicted to similarly affect each of the catchments. For example, under the IPCC-defined medium-emissions scenario SRES-A1B (Nakicenovic et al., 2000), UK Met Office Climate Predictions (Jenkins et al., 2010) indicate that, for the time period 2070-2099, average monthly rainfall within each catchment could increase by more than 20% relative to modern conditions, with much of this increase occurring during winter months. With the aim to inspect the impact of rainfall and air temperature on soil erosion over the current century, first, to understand the general behaviour, we adopted regular increments for rainfall (from -25 to +100%) and temperature (from +0 to +8°) from the baseline values (1961-1990), then, we assessed erosion rates for the periods 2010-39, 2040-69 and 2070-99 using specific future climate scenarios adopting projections from UKCP09 (UKCP09 - UK Climate Projections, 2017a, 2017b) under the IPCC (Intergovernmental Panel on Climate Change) on a defined medium CO_2 emissions scenario, SRES A1B (Special Report on Emissions Scenarios – SRES, Nakicenovic et al., 2000).

2. Materials and Methods

2.1 Summary of the modelling approach

PESERA is a spatially distributed, physically-based, continuous model created to quantify soil erosion over wide areas with different land-use types, soils, and landscape features. In PESERA, soil erodibility is a specific property that defines a soil's potential to be eroded and transported by water processes. However, the model does not differentiate between rill and interrill processes. Soil erodibility and soil crusting are associated to characteristic soil surface properties (e.g., texture, vegetation cover, and organic carbon) through the application of pedotranfer functions (Kirkby et al., 2003a; Le Bissonnais et al., 2002, 2005).

PESERA uses topography, climate, and soil characteristics to determine when rainfall intensity exceeds infiltration capacity generating runoff. Vegetation directly affects this threshold by limiting rainfall intensity through interception and increasing infiltration capacity through soil organic matter. Vegetation also functions to protect soil particles from being detached, thus reducing soil erodibility. Gross primary productivity is determined as a function of actual evapotranspiration based on empirical data (Lieth, 1975), with net primary productivity determined as the difference between gross primary productivity and temperature-driven respiration (Kirkby et al., 2008). Forests are comprised of a composite of conifers and deciduous trees, where the timing of leaf senescence is driven by changes in air temperature (Kirkby et al., 2008). The PESERA estimate of plant productivity can be seen as a maximum because the impacts of the limited availability of nutrients are not considered. Any enhancement in primary productivity could result in an exhaustion of nutrients within the rooting zone, thereby limiting vegetation growth in the long-term (Reich et al., 2014). In its implementation, PESERA iterates model runs integrating vegetation-growth dynamics and a soil-water balance until a temporally stable output between rainfall, soil, and vegetation growth is generated. The implementation also assumes that daily rainfall amounts follow a gamma distribution, which is defined using empirical data described below and a probability density function based on input precipitation values to calculate daily rainfall, runoff, and erosion for all possible storm events.

We note that, in PESERA, rainfall characterization may underestimate the role of short-duration, high-intensity precipitation events in fostering surface runoff. However, the model has been calibrated against field measurements (Pan-European Soil Erosion Risk Assessment map, Kirkby et al., 2003a) that show non-linear increases in surface runoff and soil erosion with intensifying precipitation. This non-linear relationship is consistent with process-based models involving hourly rainfall rates (Nearing et al., 2005; Pruski and Nearing, 2002b). Most important to our analysis, the characterization of rainfall at daily timescales allows PESERA simulations to be directly integrated with UKCP09 predictions.

We first assessed the sensitivity of erosion to changes in rainfall and air temperature, ensuring that the ranges of rainfall and temperature changes encompassed the expected variations reported in the UKCP09 projections. We defined baseline conditions for each catchment using the UKCP09 defined baseline period, 1961-1990, with values of monthly average temperature, monthly average rainfall, and daily total rainfall derived and interpolated from available weather station data. The sensitivity analysis then involved increasing mean-monthly air temperature from 1 to 8 °C above the 1961-1990 equivalent baseline values. Mean-monthly rainfall was adjusted by a fixed percentage from -25 to +100% of the corresponding baseline values (Figure 4).

In our modelling framework, we held the spatial distribution of land cover unchanged, allowing us to directly consider specific UKCP09 projections for the SRES A1B emissions scenario during the following defined time periods: 2010-2039, 2040-2069, and 2070-2099 (Figure 2). UKCP09 climate simulations indicate probable changes in future air temperature and precipitation, and we utilised the 10th, 50th, and 90th percentiles of the outputs for each period. We used two-tailed t-tests and Kruskal-Wallis (KW) tests to quantify the significance of differences in the populations of our measurements. Kolmogorov-Smirnov (KS) tests were applied to assess the distinctiveness of measurement distributions.

2.2 Description of PESERA

Details of the modelling framework and data requirements of PESERA have been previously reported (Kirkby et al., 2003a; 2003b; 2008), but we offer a description of the modelling framework here. An initial assumption of the model is that, during overland flow, sediment is transported at a rate equal to the flow's transport capacity per unit of flow width (*T*), which can be stated as the following based on the formulation by Kirkby et al. (2008):

$$T = k_v q^2 \Lambda, \quad (1)$$

where *T* is measured in units of kg m^{-1} day^{-1}, k_v is soil erodibility of a vegetated surface with units of kg m day L^{-2}, *q* is overland flow discharge per unit of flow width with units of L m^{-1} day^{-1}, and Λ is the local slope gradient. To account for the upslope contribution to overland flow, Eq. (1) can be restated as:

$$T = k_v (rx)^2 \Lambda, \quad (2)$$

where r is the infiltration-excess runoff in units of L m^{-2} day^{-1} for each storm and *x* is the distance from the drainage divide in units of meters. The cumulative value of T that results from the frequency distribution of storm events that occur in a month can then be written as:

$$\sum T = k_v x^2 \Lambda \sum r^2. \quad (3)$$

Eq. (3) is used in a relation that allows for estimates of the hillslope-length averaged Sediment Yield (*Y*) to the slope base, or:

$$Y = \frac{\sum C_b}{x_b} = k_v x_b \Lambda_b \sum r^2 \quad (4)$$

where the unit of *Y* is kg m^{-2} day^{-1} and the subscript *b* denotes an evaluation at the hillslope base. Eq. (4) does not consider fractions of sediment stored within the hillside during soil transfer, and PESERA does not model soil transfer through the catchment network. Moreover, the equation also does not consider the range of grain sizes that can be mobilized across the hillside, effectively treating all grain sizes as equally mobile. PESERA solves Eq. (4) within a raster model of the landscape that requires spatially distributed values of k_v, estimates of local relief derived from a digital elevation model, and spatially distributed estimates of r derived from a biophysical model.

The calculation of r is based on a bucket model that states:

$$r = p(R - h), \quad (5)$$

where R is the total daily rainfall that reaches the soil surface and h is the runoff threshold or the maximum rainfall amount that can infiltrate into the soil, having unit *m*, and p is the proportion of rainfall above the runoff threshold. The value of h is determined from soil classification data and estimates of the hydrological conditions within the near surface, including surface roughness (e.g., the storage capacity of furrows), the soil water holding capacity, and soil crusting. For the hydrological conditions of the near surface, PESERA constructs a water balance for each storm event, estimating amounts of interception loss due to vegetation cover, evapotranspiration loss due to vegetation cover and climate conditions, and the loss due to the subsurface flow of infiltrated water modelled using TopModel (Beven & Kirkby, 1979).

Vegetation is explicitly modelled by PESERA, which considers both natural and crop cover, and exerts three important controls on the likelihood of soil erosion during storm events. First, the presence of vegetation cover limits the amount of rainfall that reaches the surface through interception, so that $R = R0(1 - pI)$ where $R0$ (*m*) is the rainfall above the canopy and pI is the proportion of rainfall that is intercepted. PESERA determines pI using the following:

$$pI = 1 - exp\left(-\frac{V}{5}\right), \quad (6)$$

where V is aboveground plant biomass in units of kg ha^{-1}, which dynamically evolves as a function of climatic conditions. Second, vegetation increases the organic content of soil, which increases the soil's water-holding capacity and thus the runoff threshold, h. PESERA accounts for this in its calculation of h, using the following:

$$h = bh_m + VI + \lambda O, \qquad (7)$$

where b is the proportion of bare soil, h_m is water storage within the mineral components of the soil, I is the canopy storage of intercepted water per unit of biomass, λ is water storage within the organic components of the soil per unit of mass of organic soil, having unit m, and O (kg ha^{-1}) is the mass of organic soil. And third, the presence of vegetation decreases soil erodibility, limiting rates of soil loss during a storm, and the soil erodibility of a vegetated surface (k_v) is calculated as:

$$k_v = k_0 exp\left(-\frac{\Theta}{pr_0\varepsilon}\right), \qquad (8)$$

where k_0 is the soil erodibility of the bare surface derived from soil classification data (kg m day L^{-2}), Θ is a flow-threshold for sediment entrainment (L m^{-1} day^{-1}), r_0 is the mean rainfall amount per rain day (L m^{-2} day^{-1}) and ε, with unit m, is the product of slope length and Λ. The variable k_0 is primarily a function of grain-size characteristics, with the highest values for sandy and silty soils with low clay content (Kirkby et al., 2008). The variable Θ reflects the partitioning of shear stress exerted by overland flow onto both the soil surface and vegetation. The less vegetation that is present, the greater the amount of shear stress exerted onto the soil surface and the lower the value of Θ.

The model keeps track of three important values associated with vegetation. The outline of this portion of the model is presented here; for details and supporting references, interested readers should see Kirkby et al. (2008). The change in foliar cover (c) is determined as:

$$\Delta c = (c_0 - c)e^{-0.2V}, \quad (9)$$

where c_0, the equilibrium cover, is calculated as the ratio between the actual evapotranspiration and the potential evapotranspiration. At each time-step, V is determined by adding the net primary productivity (NPP) to the previous time-step's biomass. The NPP, in turn, is calculated as:

$$NPP = GPP - \Sigma - \Omega, \quad (10)$$

where GPP is gross primary productivity, Σ is respiration, and Ω is leaf and root fall. GPP is determined as a linear function of plant water use based on available empirical data (Lieth, 1975); note, however, that these data are for NPP and, thus, the model will conservatively underestimate the amount of biomass generation. The variable Σ is determined as a function of temperature, and Ω contribute organic matter to the soil at a rate that is dependent on biomass; the soil organic matter, in turn, decays at an exponential rate dependent on temperature.

2.3 The Study Sites

The 55-km long River Conwy drains 627 km^2 of north Wales into the Irish Sea at the Conwy Estuary. The Conwy uplands extend into the Meignant Moor of Snowdonia National Park, a Special Area of Conservation designated under the European Union Habitats Directive and characterized by steep slopes and flashy discharge. The catchment elevation spans from the sea level to a maximum of about 1086 m a.s.l. (Snowdonia National Park) with an average of 286 m a.s.l.. Because of its steep slopes, it averages a gradient of about 14.7%. The average annual discharge of the River Conwy is 19 m^3 s^{-1}, with a 95% exceedance discharge of 1.4 m^3 s^{-1} and a 5% exceedance discharge of 46 m^3 s^{-1} at the Cwmllanerch gauging station (EA No. 66011) for the period 1964-2011. Climate data for the period 1961-1990 indicate an increase in rainfall from the coast to the upland borders of the catchment, from 400 to nearly 2000 mm annually. The climate data also indicate that precipitation events are most frequent during autumn (September to November) and winter months (December to February). Mean winter and summer temperatures (at sea level) are 4.9 and 15.0 ºC. UK Met Office Climate

Predictions (UKCP09, Jenkins et al., 2010) indicate that, for the period between 2070 and 2099, summer and winter temperatures across Wales will increase on average by 3.3 and 2.9 °C, with precipitation decreasing by 18.2% during summer months and increasing by 11.3% during winter months relative to 1961-1990 averages. Ordovician, Silurian and Cambrian igneous and sedimentary rocks underlie much of the Conwy catchment, which generally weather into brown podzolic soils, peats and gleys. Overall, the Conwy catchment is rural, with urban areas making up only 1.2% of the region. The dominant land use is pasture and grassland, accounting for 64% of the catchment and supporting the primary contributor to the economy, cattle and sheep farming. Over 28% of the remaining land area is managed or natural forest (Fuller et al., 2002).

The 27-km long River Ehen drains 225 km^2 of England's west coast into the Irish Sea, with headwaters in the Ennerdale Water, a deep glacial lake that also serves as a reservoir for several urban areas in the region. The catchment has an elevation ranging from the sea level to about 854 m a.s.l. with an average of 152 m a.s.l. and a mean slope of about 11%. The average annual discharge of the river is 5.2 $m^3 s^{-1}$, with a 95% exceedance discharge of 0.94 $m^3 s^{-1}$ and a 5% exceedance discharge of 11.9 $m^3 s^{-1}$ at the Braystones gauging station (EA No. 74005) for the period 1974-2011. Average annual precipitation is between 158 and 1250 mm across the catchment with much of the precipitation occurring during autumn and winter months. The mean seasonal summer to winter temperature range is approximately 10.7 oC, with a winter mean temperature of 3.8 °C and a summer mean temperature of 14.5 °C. Predictions (UKCP09, Jenkins et al., 2010) indicate that, for the period between 2070 and 2099, summer and winter temperatures across the region will increase on average by 3.4 and 2.6 °C, with precipitation decreasing by 15.7% during summer months and increasing by 20.2% during winter months relative to 1961-1990 averages. Impervious Borrowdale volcanics underlie the upper portions of the catchment, and Ordovician sedimentary rocks are found in the lower portions, forming podzolic soils, peats and gleys in the uplands and brown soils in the lowlands. Most of the catchment is comprised of pasture and grassland (55%), with arable and forested lands being equally represented, each comprising 20% of the catchment (Fuller et al., 2002). Conservation efforts have led to the end of managed forestry, thought to be a major instigator of soil erosion within the uplands of the catchment (Killeen, 2009).

The 140-km long River Dee drains 2100 km^2 of eastern Scotland into the North Sea at the Dee Estuary (Baggaley et al., 2009). The headwaters are found in the Cairngorm massif in north-eastern Scotland, which forms part of the Cairngorm National Park. The catchment's morphology, developed on an extensive moraine relief filling the length of the valley has an altitude ranging from the sea level up to about 1307 m a.s.l. with an average of 410 m a.s.l., the mean slope is about 15%. The average annual discharge of the Dee is 47.1 m^3 s^{-1}, with a 95% exceedance discharge of 8.75 m^3 s^{-1} and a 5% exceedance discharge of 95.4 m3 s-1 at the Park gauging station (SEPA No. 12002) for the period 1972-2011. The catchment receives approximately 810 to 2100 mm of precipitation annually, most of which falls in the winter months, 30% of it as snow. The mean seasonal summer-winter temperature range is 10.8ºC, with a mean winter temperature of 3.4 ºC and a mean summer temperature of 14.2 ºC (at sea level). Predictions (UKCP09, Jenkins et al., 2010) indicate that, for the period between 2070 and 2099, summer and winter temperatures across eastern Scotland will increase on average by 3.4 and 2.3 ºC, with precipitation decreasing by 10.7% during summer months and increasing by 7.4% during winter months relative to 1961-1990 averages. Heavily metamorphosed Precambrian sedimentary rocks flanked by igneous intrusive rocks of the Caledonian orogeny underlie the catchment, forming humic-iron podzolic soils in the lowlands and expansive areas of poorly drained blanket peat bogs and podzolic soils in the uplands. Most of the catchment is comprised of forest and moorland (71.2%), with pasture and grassland comprising 17.5% and arable land comprising 7.9% (Fuller et al., 2002). The uplands have been identified as being particularly susceptible to erosion due to the prevalence of peaty soils (Towers et al., 2006)..

2.4 Terrain data

Topographic information for each catchment was derived from the Landmap Digital Terrain Model, which provides photogrammetrically derived elevation-data at 5-m resolution resampled, which we resampled to 100-m to fit an affordable resolution for modelling. Data for soil characteristics of the

Conwy and Ehen catchments were obtained under license from the UK National Soil Research Institute (NATMAP1000, National Soil Map of England and Wales, 2013), and of the Dee from the James Hutton Research Institute (SIFSS, Soil Information for Scottish Soils). The soil data were used to give field capacity and saturated water capacity for each dominant soil series. At a resolution of 100-m with soils data of a lower resolution (1-km) than used in PESERA, crusting and erodibility were obtained through a conversion from soil texture (percentage of sand, silt and clay) (Baggaley, 2011; Baggaley et al., 2010).

Land cover data were obtained from the UK Centre for Ecology and Hydrology under the Land Cover Map 2000 (LCM2000) based on Landsat image data. Most of each of the catchments is covered by forest or grassland, providing a permanent cover of the soil surface throughout the year. Agricultural crops consist of vegetables, forage, and other minor cultures such as root crops and oilseeds. These cultures have a harvesting cycle mainly between March and August, and specific calendars for planting and harvesting have been obtained from UK Agri-Environment Offices (Table 2).

2.5 Climate

In our assessment of potential climate-change impacts, we defined the period 1961-1990 as the baseline following the UKCP09 – Observed UK climate data (1961-1990) (UKCP09, 2017a). For each catchment, precipitation data were processed for PESERA by computing monthly rainfall metrics at each rain gauge site as follows: mean monthly rainfall, mean rain per rain day, and the coefficient of variation of mean rain per rain day. Linear regressions of gauge elevation and rainfall were used to interpolate the station data between gauge sites, forming a contiguous grid across all three catchments. Rainfall gauges were grouped according to elevation (0-10 m; 10-100 m; 100-200 m; 200-300 m; 300-400 m & 400-500 m), and monthly and daily rainfall data were averaged across all gauges within each elevation group. These mean values for monthly and daily rainfall were then plotted against the upper value of each elevation groups (i.e. 10 m; 100 m, 200 m, 300 m; 400 m & 500 m) from which a linear regression was fitted, giving an equation linking rainfall metric (monthly or daily) to elevation. To calculate the coefficient of variation of mean rain per rain day across the whole catchment, the monthly coefficient of variation of mean rain per rain day data were first grouped into seasons (December to February – winter; March to May – spring; June to August – summer; September to November – Autumn) before being averaged across all gauges within each elevation group and plotted, as described previously. Finally, we converted gridded elevation data into monthly rainfall metrics using the regression equations described above. Mean daily temperature and the daily temperature range were calculated from the weather stations in each catchment and then standardised by recalculating them at sea level using a lapse rate of 6ºC per 1000 m. Where catchments had more than one temperature gauge, the catchments were divided into equally spaced parcels with temperature values derived from the nearest weather station.

Climate predictions of future changes were interpolated from weather station data provided by the UK Met Office and proportionally modified for the future scenarios using UKCP09 projections under the medium-emissions scenario SRES 1AB, projections are based on the UK Met Office Hadley Centre climate model HadCM3. Estimates of potential evapotranspiration across each catchment were obtained from the UK Met Office Rainfall and Evaporation Calculation System (MORECS, Hough et al., 1997).

Precipitation and temperature data for the periods 2010-2039, 2040-2069, and 2070-2099 were obtained from the 25 km-grid UK Climate Predictions (UKCP) User Interface (UK Climate Predictions 2012, Figure 2) for each calendar month under the SRES A1B emissions scenario. In particular, data were downloaded for each calendar month under the low, medium and high emissions scenarios and at the 10%, 50% and 90% probability levels. Probabilistic climate projection are measures of strength of evidence in different future climate change outcomes. These measures are based on the current available evidence, encapsulating some of the uncertainty associated with projecting future climate and conventionally concerning the probability of change being less than given thresholds. (Murphy et al., 2010). The resolution of UKCP predictions are 40 km^2, and so each 100-m^2 grid square of each catchment was attributed to the correct UKCP grid number using the extract value to points tool in ArcGIS. The nearest land predictions were used for parcels of land within UKCP09 grid squares that were predominantly ocean. Temperature data were standardised using a lapse rate of 6ºC per 1000 m. The absolute change values from the UKCP-09 data were then added to the baseline values for precipitation and temperature. No change was made to the coefficient of rainfall per rain day values since the monthly and daily rainfall values had all been manipulated by exactly the same amount the degree of change remained constant. Temperature range was adjusted using the absolute change values for minimum and maximum daily temperatures.

2.6 Sensibility Analysis implementation

Temperature and rainfall increments were examined using an experimental framework, combining temperatures ranging from 0 to 8 °C and rainfall variations from -25 to +100% compared to the baseline values (i.e., averages of 1961/1990 dataset). It should be noted that this combination attempts to represent and explore how the PESERA models react to a systematic change of these two variables and is not used for climatic modelling of the area (Figure 4). Within the charts, dots indicate the points related to the effective rainfall temperature combination of the three climatic scenarios derived from UKCP09 SRES-A1B simulations. The procedure is useful to observe the reaction of the model, explore values other than those from real simulated scenarios, and to test different feedbacks in the context of climate and vegetation type.

3. Results and Discussion

3.1 Retrospective

The assessment of soil erosion by modelling remains a complex exercise due to uncertainty of the outputs, result validation (Alewell et al., 2019; Batista et al., 2019; Boardman, 2018; Evans & Brazier, 2005; Evans et al., 2016; Nearing, 2011), and the models behaviour in simulating hydrological fluxes (Baartman et al., 2020; Eekhout & De Vente, 2019). In addition to inspecting PESERA's capabilities under the climate change constraints, some reflections should be directed to the previous soil erosion observations, when possible, in areas close to the catchments we modelled. The intention is to provide support, even if marginal, as an ideal validation of our results.

The main concern is scarcity of specific observations within the studied catchments as well as the availability of direct monitoring at the basin scale. Nevertheless, Great Britain presents consistent literature on soil erosion and a rich dataset of soil erosion observations, which has been collected since the 1960s using a wide range of methodologies on various spatial and temporal scales (Boardman, 2006, 2013; Boardman et al., 1990; Boardman & Evans, 2006, 2019; Brazier, 2004; Evans, 1995, 2005; Evans et al., 2016, 2017). In situ observations over long periods have been performed in several programs. For instance, studies, such as the regional Soil Survey of England and Wales (SSEW, 1982-1986), Soil Survey and Land Research Centre (SSLRC, 1996-1998) on the location of the National Soil Inventory (NSI), and Agricultural Development and Advisory Service (ADAS, 1989-1994), have constituted some of the largest efforts in quantifying soil erosion nationwide until now (Boardman, 2002; Evans, 2005).

Recent works inventoried Great Britain erosion data to improve the understanding of the phenomenon. Benaud et al. (2020) realised a web-based, open-access, interactive geodatabase from previous records of soil erosion, which is at now available and integrable by users (i.e., https://piabenaud.shinyapps.io/SoilErosionMap), that undoubtedly provides excellent support to collect past and future data as support for modelling validations. For a general reference of the phenomenon, a total of 1566 individual records across Great Britain have reported soil loss averages of 1.27 and 0.72 t ha^{-1} y^{-1} for arable and grassland, respectively. In addition, Graves et al. (2015) grouped erosion values from the available national datasets for the principal soilscapes of Great Britain and determined erosion averages of 1.0 to 22.4, 0.05 to 0.75, and 0.01 to 0.5 t ha^{-1} y^{-1} in different soil textures of arable land, grasslands, and forestry, respectively. Similar values were summarized by Rickson et al. (2014) based on reports of Brazier (2004) and Brazier et al. (2012), providing rates of erosion from hillslope to the large catchment scale from various soil/land use combinations. Erosion data generally have a wide distribution of values (by one order of magnitude), and significant temporal trends have not been clearly identified by the numerous field observations over the country. Nevertheless, an increase in flooding due to land use changes have been recorded, such as in the case of observations of S-E England (South Downs) collected over 25 years

(Boardman, yrs. 1976-2001) (Boardman, 2003; Evans & Boardman, 2003). In general, even if the erosion is supposed to increase in the future because of increased rainfall (Burt et al., 2016) due to climate change (Boardman & Favis-Mortlock, 2001; Mullan et al., 2012), there are a multitude of other factors that make it difficult to understand this phenomenon such as changes in land use and crops that increase erosive cultures meant to increase soil loss (Boardman et al., 2009; Evans, 2002), changes to farm management modifying sediment redistribution (Collins and Anthony, 2008; Evans, 2006a) or changes in the timing of crop planting from spring to autumn. A report of state-of-the-art observations as support for erosion modelling activities is given by Evans et al. (2016).

To the best of our knowledge, there have been a few observations close to our study sites. For instance, in Cumbria County (Ehen catchment), Brazier (2004), from previous studies done by the Agricultural Development and Advisory Service in collaboration with the Soil Survey of England and Wales (1982-86), founded averages of about 0.22 t ha^{-1} y^{-1} in medium and light sandy loams, while Skinner and Chambers (1996), and similarly, Evans (1993) and Boardman (2013), reported rates of 1.5 m^3 ha^{-1} for a four-year record.

The available information for Northern Wales (Conwy catchment) is, for the most part, referred to as the extensive grassland of the region. For instance, James et al. (1998) estimated annual soil loss ranging 0-2.7 t ha^{-1} y^{-1} from grassland in Clwydian Hill using plot simulations. McHug (2007) and McHug et al. (2002) observed general increases in highlands of Wales and England fields and no changes in erosion for sites of northern Wales based on with data collected from 1997-1999 and 2001-2002.

Much of what we know about erosion rates on agricultural land in Eastern Scotland (Dee catchment) comes from individual studies (Davidson et al., 2001). Watson and Evans (2008) obtained large distribution values with a median of about 2.5 m^3 ha^{-1} from several years of field observations in agricultural lowlands. Rickson et al. (2019) utilized Scottish Environment Protection Agency (SEPA) surveys on 10 selected catchments and summarized previous datasets to estimate erosion rates of 0.01-23.0 t ha^{-1} yr^{-1} in arable areas of Scotland in addition to soil losses of 0.13-0.33, 0.07-0.12, and 0.04-0.07 mm yr^{-1} for arable land, rough grassland, and forests, respectively.

3.2 Modelling results

Our modelling results, under baseline conditions, determined average soil erosion rates of 0.24 and 0.28 t ha^{-1}yr^{-1} for Conwy and Ehen catchments, respectively (Figure 3, Table 3). The Dee catchment experienced higher rates of soil loss, with a catchment-wide average soil erosion rate equal to 0.65 t ha^{-1}yr^{-1} due to the prevalence of highly erodible soils within steep catchment margins. Model results under baseline conditions also reveal the importance of land cover in soil loss. In all cases, average soil erosion rates for forests and grasslands were significantly less than those for arable lands (t-tests: α=0.05; KW: α=0.05). KS tests further confirm that the distribution of soil erosion rates for arable lands differs from forests and grasslands (α<0.05) in all catchments.

On average, PESERA predicts that forests, grasslands, and arable lands yield 0.36, 0.26, and 1.09 t ha^{-1}yr^{-1} of soil during baseline conditions (Table 3). Values obtained for soils of forests, grassland, and arable land in Conwy, Ehen, and Dee catchments were determined to be 0.20, 0.22, 1,17; 0.25, 0.23, 0.48; and 0.62, 0.32, 1.62 t ha^{-1}yr^{-1}, respectively.

In climatic projections for 2010-2039, 2040-2069, and 2070-2099 (Figure 4, Table 3), all the catchments show, at the 10th and 50th percentiles, values lower or slightly lower than the baseline (from 0.17 to 0.21, 0.22 to 0.28 and 0.44 to 0.66, t ha^{-1}yr^{-1}, for the Conwy, Ehen and Dee, respectively). At the 90th percentile, the Conwy catchment still holds values close to the baseline (0.23 to 0.25 t ha^{-1} yr^{-1}), while Ehen and Dee are higher than the reference (0.34 to 0.45 and 0.90 to 0.95 t ha^{-1}yr^{-1}, respectively).

Sensitivity analyses of testing temperature changes from 0 to 8 °C and rainfall variations from -25% to +100% reveal specific erosion trends, proportional to rainfall and inversely proportional to temperature risings (Figure 4). Globally, the values span from a minimum of 0.02 in Conwy to a maximum of 3.26 t ha^{-1}y^{-1} in Dee (Figure 5a) with variations from the baseline ranging from -90% to +402.9% (Figure 5b).

3.3 General considerations

The sensitivity analysis reveals that the three catchments have similar responses to the variations of climatic parameters (Figures 4 and 5): 1) The erosion rate displays a growing trend proportional to increasing rainfall, which is less evident in the Conwy and more pronounced in the Ehen and Dee, 2) A reduction effect of temperature on soil loss is observed in the Conway and Ehen catchments most likely due to vegetation production, but less evident in Dee as detailed below.

Regarding impacts of incremental increases in rainfall on soil erosion but at baseline temperature (i.e., temperature increment = 0) (Figure 5b), we note a minor effect across the Conwy catchment (from 0 to 213.5%), an average response across the Ehen (from -24.1 to 315.1%), and a maximum influence across the Dee (from -24.5 to 379.5%), which appears to result from the integrative effects of different land uses. Forest and grassland, the most mitigating surfaces, are dominant (92%) in the Conway, where there are also limited crops (1.8%), and thus can contribute to reduced erosion. In contrast, crops can enhance the effect across the Dee as they comprise 7.2% of the land surface.

Temperature also has a contribution in reducing erosion. At baseline rainfall values (Figure 5b) (i.e., rainfall increment = 0), increases in temperature can reduce erosion to -45.5, -36.8, and -24.2% for the Conwy, Ehen, and Dee, respectively.

When erosion reduction is calculated respect to the baseline temperature within each relative rainfall increment (Figure 5c), it is still the greatest in the Conwy (from -90% at -25% rainfall to -28.5% at +100% rainfall), has an average effect in the Ehen (from -32.7% at -25% rainfall to -18.9% at +100% rainfall), and exerts a more constraining effect in the Dee (from -30% at -25% rainfall to 2.8% at +100% rainfall). This influence is more evident in the Conwy and Ehen due to the vegetation productivity of forest and grassland, which respectively comprise a total of 92% and 94% of the surface compared to 88% in the Dee catchment.

Based on our results, temperature growth can compensate for the increased erosion that would have otherwise been generated through increases in rainfall. As shown in Figure 5b, a reversal point is detected at 25% rainfall between 4-6 °C in the Conwy, at +5% rainfall between 0-1°C in the Ehen, and at +5% rainfall between 2-4°C in the Dee. The difference is still due to the effect of the higher percent of forest and grassland in the Conwy and Ehen than in the Dee.

Generally, the sensitivity analysis reveals the potential role of vegetation in limiting rates of soil loss caused by increased rainfall. Each catchment is capable of experiencing reduced rates of soil loss relative to baseline conditions when the increased rainfall is associated with higher air temperatures. If primary productivity is not limited by nutrient availability or soil moisture, then sustained increases in air temperature should lead to greater vegetation cover, requiring more rainfall to accelerate soil loss. Temperature-driven increases in aboveground biomass decrease the likelihood of infiltration-excess runoff because of the associated increases in both rainfall interception and the soil's water-holding capacity (Routschek et al., 2014).

3.4 Land use influence

In conjunction with a decrease in soil erodibility caused by the enriched biomass, these effects can lead to a potential negative-feedback mechanism that can limit climate-driven soil loss, but only where vegetation cover persists throughout the year. Forests and grasslands, which comprise a greater proportion of the land surface of all catchments, appear relatively resilient to increased rainfall, where any associated increases in air temperature generally reduce changes in erosion (Figure 4, a and b). Conversely, large surfaces of arable lands can be more reactive to rainfall changes with a lower response to increases in temperature (Figure 4c). These behaviours are well observed in charts for different land uses, as shown in Figure 6, where the threshold line is shifted to the right in grassland and forest (towards high rainfall - high temperatures), with no substantial effect from high temperatures on arable lands.

The negative feedback provided by forests and grasslands should be limited during winter months, when aboveground biomass is reduced and rainfall is more intense. Seasonal patterns in soil loss across arable lands are more sensitive to agricultural cycles associated with particular crops, which will define the time periods when arable lands are fallow. Arable lands will thus require mitigation strategies to minimize soil loss during fallow periods when vegetation cover is minimal or absent.

3.5 Climatic scenarios effect

Mapping the UKCP09 projections for the IPCC medium-emissions scenario SRES A1B onto the results of the sensitivity analysis (Figures 4 and 6) reveals perhaps the most important implication of our findings. UKCP09 projections indicate that future climate changes may involve consistent changes in average-monthly rainfall and average-annual air temperatures. Consequently, moving through the 2010-39, 2040-69, and 2070-99 projections, we observe some differences between the erosion response of the catchments (Figure 4, Table 3). For the Conwy, we report a decrease of erosion rate at all the percentile levels (from 4.2 to -33%), which is more consistent at the 10^{th} percentile. In the Ehen, a slight decrease in erosion (from 0 to -28.6%) is detected at the lower percentiles (10^{th} and 50^{th}), while an increase is observed from 21.4 to 60.7% at the 90^{th} percentile. The Dee catchment has a similar behaviour, but with a more consistent decrease for the 10^{th} and 50^{th} percentiles (from 1.5 to -35.8%) and higher erosion rates for the 90^{th} percentile (from 31.1 to 46.2%). Over the statistical framework of the climatic scenario projections, it is reasonable to say that, considering the 90^{th} percentile as the more "inclusive" of the climatic predictions, a generalised future decrease of the erosion rates is verified in the Conwy catchment, while an increase is identified for the Ehen and Dee.

Critical to our findings is that patterns of land use is the principal variable determining the varying responses to climate change between the catchments. Forest and grassland are responsible for a decreasing or stationary change in erosion rates, more pronounced for the Conwy and less marked in the Ehen and Dee. In the Dee, more erodible soils due to topography cause a slightly different response, but the effect of arable lands associated with increased erosion are present in almost all projections, especially in the Ehen and Dee catchments starting from 50th and 90th percentiles. Although the manner by which vegetation will respond to climate change remains unclear (Arneth, 2015, Davies-Barnard et al., 2015), including a possible expansion of arable lands (Adams et al., 1990; Nelson et al., 2014), our findings indicate the potential of climate change to reduce soil loss by enhancing primary productivity. Our results, illustrating the potential impacts of climate change on vegetation growth, are comparable to previous assessments (Bull, 1991; Melillo et al., 1993; Acosta et al., 2015). Moreover, the negative-feedback mechanism that we observed may be pervasive throughout permanently vegetated environments, given that soil erosion can occur due to a range of processes that can be limited by enhanced primary productivity (e.g., rain splash, debris flow).

4. Conclusions

The objective of this research was to verify the impact of climate change and vegetation on soil erosion in three catchments by the way of a sensitivity analysis as modelled by the Pesera. For that, with adopted a systematic implementation of changes of temperature and rainfall to acknowledge general behaviour of the model, then, we assessed the impact on erosion using the climatic projection from UKCP09 at the horizons 2010-39, 2040-69 and 2070-99. The results of the modelling suggest that an increasing in rainfall has a direct and positive effect on erosion, while temperature rise can mitigate runoff and erosion. Current evidence suggests that climate change is increasing net primary productivity (Nemani et al., 2003; Buermann et al., 2016; Ballantyne et al., 2017) with the potential for increased water usage (Frank et al., 2015; Berg et al., 2016) and vegetation cover on a global scale (Betts et al., 1997). Based on our findings, the presented modelling work is in line with these observations and highlights the potential impacts of climate change on soil erosion due to overland flow.

In areas with permanent vegetation cover, climate change could reduce the likelihood of overland flow by increasing interception losses and infiltration rates. Increases in below-ground biomass would also reduce soil erodibility. This effect is evident when arable lands and forest/grassland are compared: forest and grasslands are highly affected by primary vegetation productivity, mitigating the impact of climatic change (i.e., increased rainfall and temperature) on soil erosion; while arable lands are less influenced by the vegetation productivity effect due to their annual agricultural cycle. That said, there are three important issues should be further addressed regarding our findings.

First, plant growth in our modelling approach is driven primarily by air temperature and does not consider increases in atmospheric CO_2, which may end up improving plant water-use efficiency (Van der Sleen et al., 2015). Second, our use of daily rainfall in assessing precipitation may be too coarse to adequately document the impacts of short-lived, high-intensity events. Although predictions of hourly and sub-hourly rainfall resulting from climate change may be speculative, advances in modelling performance provide an opportunity to assess the impacts of rainfall extremes (Kendon et al., 2014). And finally, our approach does not consider sustained shifts in land cover that may result directly (Eigenbrod et al., 2015) or indirectly (Nelson et al., 2014) from climate change. Nevertheless, our results confirm the potentially negative feedback of the function of plants in the environment as implemented in the model. Indeed, the results verify the importance of both conserving and expanding vegetation cover to improve the landscapes' ability to withstand the impacts of climate change on widespread soil loss.

Acknowledgments, Samples, and Data

We thank Emmanuel Gabet, Loraine Whitmarsh, Nikki Baggaley, and Elizabeth B. Kendon for assistance in hypothesis development and data collection. The study was supported by an ESRC/NERC Interdisciplinary Research Studentship to K. Walker-Springett (ES/I004165/1) and funding from the Climate Change Consortium of Wales for R. Ciampalini. J.A.C. and S.J.O. conceived of the study. R.C. and K.W.-S. compiled baseline data and conducted model simulations. T.C.H. and I.R.H. assisted in hypothesis development and provided expertise in climate-change impacts and soil erosion. R.C., K.W.-S. and J.A.C. led data analysis and interpretation, assisted by all co-authors. J.A.C. drafted the paper, which was then reviewed by all co-authors. The authors declare no competing financial interests. A special appreciation is addressed to the reviewers who, in the different phases of this editorial realization, provided constructive contributions that largely aided the completion of this article in the right direction.

References

Acosta, V.T., T.F. Schildgen, B.A. Clarke, D. Scherler, B. Bookhagen, H. Wittmann, F. von Blanckenburg, & Strecker, M.R., 2015. Effect of vegetation cover on millennial-scale landscape denudation rates in East Africa. Lithosphere 7, 408-420. doi: 10.1130/L402.1.

Adams, R.M., C. Rosenzweig, R.M. Peart, J.T. Ritchie, B.A. McCarl, J.D. Glyer, R.B. Curry, J.W. Jones, K.J. Boote, & Allen Jr., L.H., 1990. Global climate change and US agriculture. Nature 345, 219-224. doi: 10.1038/345219a0.

Alewell, C., Borrelli, P., Meusburger, K., & Panagos, P. (2019). Using the USLE: Chances, challenges and limitations of soil erosion modelling. International Soil and Water Conservation Research 7 (3), 203–225. doi:10.1016/j.iswcr.2019.05.004.

Arneth, A., 2015. Uncertain future for vegetation cover. Nature 524, 44-45. doi: 10.1038/524044a.

Baartman, J. E. M., Nunes, J. P., Masselink, R., Darboux, F., Bielders, C., Degre, A., Cantreul, V., Cerdan, O., Grangeon, T., Fiener, P., Wilken, F., Shindewolf, M., Wainwright, J., 2020. What do models tell us about water and sediment connectivity? Geomorphology 107300. doi:10.1016/j.geomorph.2020.107300.

Baggaley, N., 2011. Discussion regarding use of PESERA model, James Hutton Research Institute, Aberdeen.

Baggaley, N., Langan, S.J., Futter, M.N., Potts, J.M., and Dunn, S.M., 2009. Long-term trends in hydro-climatology of a major Scottish mountain river. Science of the Total Environment 407, 4633-4641. https://doi.org/10.1016/j.scitotenv.2009.04.015.

Baggaley, N., Lilly, A., Walker, R., Castellazzi, M., 2010. An assessment of the data resolution required to run the PESERA soil erosion model at a catchment scale in a high latitude agricultural catchment, 19th World Conference of Soil Solutions for a Changing World, Brisbane, Australia.

Baggaley, N., Potts, J., 2017, Sensitivity of the PESERA soil erosion model to terrain and soil inputs. Geoderma Regional 11,104-112.

Ballantyne, A., Smith, W., Anderegg, W., Kauppi, P., Sarmiento, J., Tans, P., Shevliakova, E., Pan, Y., Poulter, B., Anav, A., Friedlingstein, P., Houghton, R. & Running, S., 2017. Accelerating net terrestrial carbon uptake during the warming hiatus due to reduced respiration. Nature Climate Change 7, 148-152. doi:10.1038/nclimate320.

Batista, P. V. G., Davies, J., Silva, M. L. N., & Quinton, J. N., 2019. On the evaluation of soil erosion models: Are we doing enough? Earth-Science Reviews 102898. doi:10.1016/j.earscirev.2019.102898.

Benaud, P., Anderson, K., Evans, M., Farrow, L., Glendell, M., James, M.R., Quine, T.A., Quinton, J.N., Rawlins, B., Rickson, R.J., Brazier, R.E., 2020. National-scale geodata describe widespread accelerated soil erosion. Geoderma 371, 114378. doi:10.1016/j.geoderma.2020.114378.

Berg, A., et al., 2016. Land–atmosphere feedbacks amplify aridity increase over land under global warming, Nature Climate Change 6, 869. doi:10.1038/nclimate3029.

Betts, R.A., Cox, P.M., Lee, S.E. & Woodward, F.I., 1997. Contrasting physiological and structural vegetation feedbacks in climate change simulations. Nature 387, 796-799.

Beven, K.J. & Kirkby, M.J., 1979. A physically based, variable contributing area model of basin hydrology. Hydrol. Sci. Bull. Sci. Hydrol. 24, 1-3.

Boardman, J., 2002. The Need for Soil Conservation in Britain: Revisited. Area 34, 419–427. https://doi.org/10.2307/20004273.

Boardman, J., 2003. Soil erosion and flooding on the eastern South Downs, southern England, 1976-2001. Transactions of the Institute of British Geographers 28(2), 176–196. doi:10.1111/1475-5661.00086.

Boardman, J., 2006. Soil erosion science: Reflections on the limitations of current approaches. Catena 68 (2-3), 73–86. doi:10.1016/j.catena.2006.03.007.

Boardman, J., 2013. Soil Erosion in Britain: Updating the Record. Agriculture 3, 418-442, doi:10.3390/agriculture3030418.

Boardman, J., 2018. The Challenge of Soil Erosion: Where Do We Now Stand? Int. J. Environ. Sci. Nat. Res. 15 (1), 24-26. doi:10.19080/IJESNR.2018.15.555904.

Boardman, J., Evans, R., Favis-Mortlock, D. T., & Harris, T. M., 1990. Climate change and soil erosion on agricultural land in england and wales. Land Degradation and Development 2 (2), 95–106. doi:10.1002/ldr.3400020204.

Boardman, J., & Evans, B., 2006. Britain. In “Soil Erosion in Europe”. Wiley & Sons Ltd, 439–453. doi:10.1002/0470859202.ch33.

Boardman, J., & Evans, R., 2019. The measurement, estimation and monitoring of soil erosion by runoff at the field scale: Challenges and possibilities with particular reference to Britain. Progress in Physical Geography: Earth and Environment, 030913331986183. doi:10.1177/0309133319861833.

Boardman, J. & Favis-Mortlock, D.T. 1993. Climate change and soil erosion in Britain. The Geographical Journal. 159(2), 179-183, doi: 10.2307/3451408.

Boardman, J., & Favis-Mortlock, D.T., 2001. How will Future Climate Change and Land-Use Change Affect Rates of Erosion on Agricultural Land? Research for the 21st Century, Proc. Int. Symp. (3-5 January 2001, Honolulu, HI, USA). Eds. J.C. Ascough II and D.C. Flanagan. St. Joseph, MI: ASAE.701P0007.

Boardman, J., Shepheard, M. L., Walker, E., & Foster, I. D. L., 2009. Soil erosion and risk-assessment for on- and off-farm impacts: A test case using the Midhurst area, West Sussex, UK. Journal of Environmental Management 90 (8), 2578–2588. doi:10.1016/j.jenvman.2009.01.018.

Borselli L., Salvador Sanchism. P., Batolini D., Cassi P., Lollino P., 2011. PESERA-L model: an addendum to the PESERA model for sediment yield due to shallow mass movement in a watersheed. CNR-IRPI, Italy Report n. 82. Scientific report deliverable 5.2.1, DESIRE PROJECT. EU FP6 DESIRE project P.28.

Brazier, R., 2004. Quantifying soil erosion by water in the UK: a review of monitoring and modelling approaches. Progress in Physical Geography 28 (3), 340–365. doi:10.1191/0309133304pp415ra.

Brazier R, Anderson K, Bellamy P, Ellis M, Evans M, Quine T, Quinton JN, Rawlins B, Rickson RJ., 2012. Developing a cost-effective framework for monitoring soil erosion in England and Wales. Final Report to Defra: Project SP1303.

Buermann, W., Beaulieu, C., Parida, B., Medvigy, D., Collatz, G.J., Sheffield, J. & Sarmiento, J.L., 2016. Climate-driven shifts in continental net primary production implicated as a driver of a recent abrupt increase in the land carbon sink. Biogeosciences 13, 1597-1607. doi: 10.5194/bg-13-1597-2016.

Bull, W.B., 1991. Geomorphic Responses to Climate Change. Oxford University Press, 326p.

Burt, T., Boardman, J., Foster, I., & Howden, N., 2016. More rain, less soil: long-term changes in rainfall intensity with climate change. Earth Surface Processes and Landforms 41(4), 563-566, doi:10.1002/esp.3868.

Cheviron B., S.J. Gumiere, Y. Le Bissonnais, Raclot, D., and Moussa, R., 2010. Sensitivity analysis of distributed erosion models - framework. Water Resour. Res. 46, W08508.

Cheviron B., Le Bissonnais, Y., Desprats, J.F., Couturier, A., Gumiere, S.J., Cerdan, O., Darboux, F. and Raclot, D., 2011. Comparative sensitivity analysis of four distributed erosion models, Water Resour. Res. 47, W01510.

Collins, A.L., & Anthony, S.G., 2008. Assessing the likelihood of catchments across England and Wales meeting "good ecological status" due to sediment contributions from agricultural sources. Environmental Science & Policy 11 (2), 163–170. doi:10.1016/j.envsci.2007.07.008.

Cooksley, S.L., Brewer, M.J., Donnelly, D., Spezia, L. & Tree, A., 2012. Impacts of artificial structures on the freshwater pearl mussel Margaritifera margaritifera in the River Dee, Scotland. Aquatic Conservation 22, 318-330. doi: 10.1002/aqc.2241.

Cramer, W., Bondeau, A., Woodward, F.I., Prentice, I.C., Betts, R.A., Brovkin, V., Cox, P.M., Fisher, V., Foley, J.A., Friend, A.D., Kucharik, C., Lomas, M.R., Ramankutty, N., Sitch, S., Smith, B., White, A., & Young-Molling, C., 2001. Global response of terrestrial ecosystem structure and function to CO2 and climate change: results from six global vegetation models. Global Change Biology 7, 357-373. doi: 10.1046/j.1365-493 2486.2001.00383.x.

Davidson, D.A., Grieve, I.C., & Tyler, A.N., 2001. An Assessment of Soil Erosion by Water in Scotland. The GeoJournal Library 93–108. doi:10.1007/978-94-017-2033-5_6.

Davies-Barnard, T., Valdes, P. J., Singarayer, J. S., Wiltshire, A. J., Jones, C. D., 2015. Quantifying the relative importance of land cover change from climate and land use in the representative concentration pathways. Global Biogeochemical Cycles 29 (6), 842-853. doi.org/10.1002/2014GB004949.

De Vente, J., Poesen., J., Verstraeten., g., Van Rompaey, Govers., G., 2008. Spatially distributed modelling of soil erosion and sediment yield at regional scales in Spain. Global and Planetary Change 60, 393–415.

Eekhout, J. P. C., & De Vente, J., 2019. How soil erosion model conceptualization affects soil loss projections under climate change. Progress in Physical Geography: Earth and Environment 030913331987193. doi:10.1177/0309133319871937.

Eigenbrod, F., P. Gonzalez, J. Dash, and Steyl, I., 2015. Vulnerability of ecosystems to climate change moderated by habitat intactness, Global Change Biology 21 (1), 275-286. doi:10.1111/gcb.12669.

Esteves, T. C. J., Kirkby, M. J., Shakesby, R. A., Ferreira, A. J. D., Soares, J. A. A., Irvine, B.J., Ferreira, C.S.S., Coelho, C.O.A., Bento, C.P.M., Carreiras, M.A., 2012. Mitigating land degradation caused by wildfire: Application of the PESERA model to fire-affected sites in central Portugal. Geoderma 191, 40–50.

Evans, R., 1993. Extent, frequency and rates of rilling of arable land in localities in England and Wales. In: Wicherek S (ed.) Farm Land Erosion in Temperate Plains Environment and Hills. Amsterdam: Elsevier, 177–190.

Evans, R., 1995. Some methods of directly assessing water erosion of cultivated land - a comparison of measurements made on plots and in fields. Progress in Physical Geography 19 (1), 115–129. doi:10.1177/030913339501900106.

Evans, R., 2002. An alternative way to assess water erosion of cultivated land – field-based measurements: and analysis of some results. Applied Geography 22 (2), 187–207. doi:10.1016/s0143-6228(02)00004-8.

Evans, R., 2005. Monitoring water erosion in lowland England and Wales—A personal view of its history and outcomes. Catena 64 (2-3), 142–161. doi:10.1016/j.catena.2005.08.003.

Evans, R., 2006. Land use, sediment delivery and sediment yield in England and Wales. In: Owens PN, Collins AJ, editors. Soil Erosion and Sediment Redistribution in River Catchments. Wallingford: CAB International, p. 70–84.

Evans, R., & Boardman, J., 2003. Curtailment of muddy floods in the Sompting catchment, South Downs, West Sussex, southern England. Soil Use and Management 19 (3), 223–231. doi:10.1111/j.1475-2743.2003.tb00308.x.

Evans, R., & Boardman, J., 2016. The new assessment of soil loss by water erosion in Europe. Panagos P. et al., 2015 Environmental Science & Policy 54, 438–447—A response. Environmental Science & Policy 58, 11–15, doi:10.1016/j.envsci.2015.12.013.

Evans, R., & Brazier, R., 2005. Evaluation of modelled spatially distributed predictions of soil erosion by water versus field-based assessments. Environmental Science & Policy, 8 (5), 493–501. doi:10.1016/j.envsci.2005.04.009.

Evans, R., Collins, A. L., Foster, I. D. L., Rickson, R. J., Anthony, S. G., Brewer, T., Deeks, L., Newell-Price, J.P., Truckell, I.G., & Zhang, Y., 2016. Extent, frequency and rate of water erosion of arable land in Britain - benefits and challenges for modelling. Soil Use and Management 32, 149–161. doi:10.1111/sum.12210.

Evans, R., Collins, A.L., Zhang, Y., Foster, I.D.L., Boardman, J., Sint, H., Lee, M.R.F., Griffith, B.A., 2017. A comparison of conventional and 137 Cs-based estimates of soil erosion rates on arable and grassland across lowland England and Wales. Earth-Science Reviews 173, 49–64. doi:10.1016/j.earscirev.2017.08.005

Favis-Mortlock, D. & Boardman, J., 1995. Nonlinear responses of soil erosion to climate change: a modelling study on the UK South Downs. Catena 25(1-4), 365-387, doi.org/10.1016/0341-8162(95)00018-N.

Fleskens., L., Kirkby, M.J., Irvine, B.J., 2016. The PESERA-DESMICE Modeling Framework for Spatial Assessment of the Physical Impact and Economic Viability of Land Degradation Mitigation Technologies. Front. Environ. Sci. 4:31. doi: 10.3389/fenvs.2016.00031.

Frank, D. C., et al., 2015. Water-use efficiency and transpiration across European forests during the Anthropocene, Nature Climate Change 5, 579. doi:10.1038/nclimate2614.

Fuller, R.M., Smith, G.M., Sanderson, J.M., Hill, R.A., Thomson, A.G., Cox, R., Brown, N.J., Clarke, R.T., Rothery, P., Gerard, F.F., 2002. Land Cover Map 2000: A guide to the classification system, Centre for Ecology and Hydrology, Cambridgeshire, UK.

Galy, V., Peucker-Ehrenbrink, B. & Eglinton, T., 2015. Global carbon export from the terrestrial biosphere controlled by erosion. Nature 521, 204-207, doi:10.1038/nature14400.

Garbrecht, J. D. & Zhang, X.C., 2015. Soil erosion from winter wheat cropland under climate change in central Oklahoma. Applied Engineering in Agriculture 31(3), 439-454.

Gedney, N., Cox, P.M., Betts, R.A., Boucher, O., Huntingford, C. & Stott, P.A., 2006. Detection of a direct carbon dioxide effect in continental river runoff records. Nature 439, 835-838.

Geist, J. & Auerswald, K., 2007. Physicochemical stream bed characteristics and recruitment of the freshwater pearl mussel (Margaritifera margaritifera). Freshwater Biology 52, 2299-2316, doi: 10.1111/j.1365-2427.2007.01812.x.

Graves, A.R., Morris, J., Deeks, L.K., Rickson, R. J., Kibblewhite, M.G., Harris, J.A., Farewell, T.S., Truckle, I., 2015. The total costs of soil degradation in England and Wales. Ecological Economics 119, 399–413. doi:10.1016/j.ecolecon.2015.07.026.

Guo, Y., Peng, C., Zhu, Q., Wang, M., Wang, H., Peng, S., & He, H., 2019. Modelling the impacts of climate and land use changes on soil water erosion: Model applications, limitations and future challenges. Journal of Environmental Management 250, 109403. doi:10.1016/j.jenvman.2019.109403.

Hairsine, P.B. & Rose, C.W., 1992. Modeling water erosion due to overland flow using physical principles 1. Sheet flow. Water Resources Research 28, 237-243, doi: 10.1029/91WR02380.

Nakicenovic, N., Alcamo, J., Grubler, A., Riahi, K., Roehrl, R.A., Rogner, H-H., & Victor N (2000). Special Report on Emissions Scenarios (SRES), A Special Report of Working Group III of the Intergovernmental Panel on Climate Change. Cambridge: Cambridge University Press, ISBN 0-521-80493-0.

IPCC, 2019: Climate Change and Land: an IPCC special report on climate change, desertification, land degradation, sustainable land management, food security, and greenhouse gas fluxes in terrestrial ecosystems [P.R. Shukla, J. Skea, E. Calvo Buendia, V. Masson-Delmotte, H.-O. Pörtner, D. C. Roberts, P. Zhai, R. Slade, S. Connors, R. van Diemen, M. Ferrat, E. Haughey, S. Luz, S. Neogi, M. Pathak, J. Petzold, J. Portugal Pereira, P. Vyas, E. Huntley, K. Kissick, M. Belkacemi, J. Malley, (eds.)]. In press.

James, P.A., Alexander, R.W., 1998. Soil erosion and runoff in improved pastures of the Clwydian Range, North Wales. J. Agric. Sci. Cambridge 130, 473-488.

Jenkins, G., Murphy, J., Sexton, D., Lowe, J., Jones, P. & Kilsby, C., 2010. UK Climate Projections: Briefing Report. Department for Environment, Food and Rural Affairs and Department of Energy and Climate Change.

Joint Nature Conservation Committee, 2007. Second Report by the United Kingdom under Article 17 on the implementation of the Habitats Directive from January 2001 to December 2006. Peterborough, JNCC.

Hough, M. N. and Jones, R. J. A., 1997. The United Kingdom Meteorological Office rainfall and evaporation calculation system: MORECS version 2.0-an overview, Hydrol. Earth Syst. Sci., 1, 227-239, doi:10.5194/hess-1-227-1997.

Karamesouti, M., Petropoulos, G.P., Papanikolaou, I.D., Kairis, O., Kosmas, K., 2016. Erosion rate predictions from PESERA and RUSLE at a Mediterranean site before and after a wildfire: Comparison & implications. Geoderma 26,144–58.

Keenan, T. F., Hollinger, D. Y., Bohrer, G., Dragoni, D., Munger, J. W., Schmid, H. P., & Richardson, A. D., 2013. Increase in forest water-use efficiency as atmospheric carbon dioxide concentrations rise. Nature 499(7458), 324–327. doi:10.1038/nature12291.

Kendon, E.J., Roberts, N.M., Fowler, H.J., Roberts, M.J., Chan, S.C., Senior, C.A., 2014. Heavier summer downpours with climate change revealed by weather forecast resolution model. Nature Climate Change 4, 570–576.

Kharin, V.V., Zwiers, F.W., Zhang, X. & Hegerl, G.C., 2007. Changes in temperature and precipitation extremes in the IPCC ensemble of global coupled model simulations. J. Climate 20, 1419-1444.

Killeen, I., 2009. Conservation and restoration of a freshwater pearl mussel (Margaritifera margaritifera) population in Northern England, in: Henrikson, L., Arvidsson, B., Österling, M. (Ed.), Aquatic Conservation with a focus on Margaritifera margaritifera. Karlstad University, Sundsvall, Sweden.

Kirkby. M.J., and the Pesera Team, 2003a. Pan-European Soil Erosion Risk Assessment: The PESERA Map, Version 1 October 2003. Explanation of Special Publication Ispra 2004 No.73 (S.P.I.04.73).

Kirkby. M.J., Gobin, A., Irvine, B., 2003b. Pan-European Soil Erosion Risk Assessment. PESERA Project, Deliverable 05: Pesera Model Strategy, Land Use and Vegetation Growth.

Kirkby, M.J., Irvine, B.J., Jones, R.J.A., Govers, G. & the PESERA team, 2008. The PESERA coarse scale erosion model for Europe. I. – Model rational and implementation. Eur. J. Soil Sci. 59, 1293-1306.

Lal, R., 2004. Soil carbon sequestration impacts on global climate change and food security. Science 304, 1623-1627.

LCM2000, 2000. Land Cover Map 2000, https://www.ceh.ac.uk/services/land-cover-map-2000.

Le Bissonnais., Y., Montier, C., Jamagne, M., Daroussin, J., King, D., 2002. Mapping erosion risk for cultivated soil in France. Catena 46, 207–220.

Le Bissonnais, Y., Cerdan, O., Lecomte, V., Benkhadra, H., Souchere, V., Martin, P., 2005. Variability of soil surface characteristics influencing runoff and interrill erosion. Catena 62, 111-124.

Li, P., Holden, J., Irvine, B., Grayso, R., 2016. PESERA-PEAT: a fluvial erosion model for blanket peatlands. Earth surface processes and landforms 41, 14, 2058-2077.

Li, Z. & Fang, H., 2016. Impacts of climate change on water erosion: A review. Earth-Science Reviews 163, 94–117.

Licciardello, F., Govers., G., Cerdan., O., Kirkby., M.J., Vacca, A., Kwaad., F.J.P.M., 2009. Evaluation of the PESERA model in two contrasting environments. Earth Surf. Process. Landforms 34, 629–640.

Lieth, H., 1975. Modeling the primary productivity of the world. In Ecological Studies – Analysis and Synthesis. Springer-Verlag 14, 237-263.

Luetzenburg, G., Bittner, M. J., Calsamiglia, A., Renschler, C. S., Estrany, J., & Poeppl, R., 2019. Climate and land use change effects on soil erosion in two small agricultural catchment systems Fugnitz - Austria, Can Revull - Spain. Science of The Total Environment 135389. doi:10.1016/j.scitotenv.2019.135389.

McHugh, M., 2007. Short-term changes in upland soil erosion in England and Wales: 1999 to 2002. Geomorphology 86 (1-2), 204–213. doi:10.1016/j.geomorph.2006.06.010.

McHugh, M., Harrod, T., & Morgan, R., 2002. The extent of soil erosion in upland England and Wales. Earth Surface Processes and Landforms 27 (1), 99–107. doi:10.1002/esp.308.

Melillo, J.M., McGuire, A.D., Kicklighter, D.W., Moore III, B., Vorosmarty, C.J. & Schloss, A.L., 1993. Global climate change and terrestrial net primary production. Nature 363, 234-240.

Meusburger, K., Konz, N., Schaub, M., Alewell, C., 2010. Soil erosion modelled with USLE and PESERA using QuickBird derived vegetation parameters in an alpine catchment. International Journal of Applied Earth Observation and Geoinformation 12 (3), 208-215.

Mullan, D., 2013. Soil erosion under the impacts of future climate change: Assessing the statistical significance of future changes and the potential on-site and off-site problems. Catena. 109, 234-246.

Mullan, D.J., Favis-Mortlock, D.T., Fealy, R., 2012. Addressing key limitations associated with modelling soil erosion under the impacts of future climate change. Agricultural and Forest Meteorology 156, 18–30.

Murphy, J.M., Sexton, D.M.H., Jenkins, G.J., Boorman, P.M., Booth, B.B.B., Brown, C.C., Clark, R.T., Collins, M., Harris, G.R., Kendon, E.J., Betts, R.A., Brown, S.J., Howard, T. P., Humphrey, K. A., McCarthy, M. P., McDonald, R. E., Stephens, A., Wallace, C., Warren, R., Wilby, R., Wood, R. A., 2010. UK Climate Projections Science Report: Climate change projections. Version 3. Met Office Hadley Centre, Exeter.

NATMAP1000, 2013. National Soil Map of England and Wales, Cranfield University.

Nearing, M.A., Hairsine, P., 2011. The Future of Soil Erosion Modelling. In: Morgan, R.P. and M.A. Nearing (eds.). Handbook of Erosion Modelling. Wiley-Blackwell Publishers, Chichester, West Sussex, UK. p. 387-397.

Nearing, M.A., Jetten, V., Baffaut, C., Cerdan, O., Couturier, A., Hernandez, M., Le Bissonnais, Y., Nichols, M.H., Nunes, J.P., Renschler, C.S., Souchere, V., van Oost, K., 2005. Modeling response of soil erosion and runoff to changes in precipitation and cover. Catena 61, 131–154.

Nearing, M.A., Pruski, F.F. & O'Neal, M.R., 2004. Expected climate change impacts on soil erosion rates: a review. J. Soil Water Conserv. 59, 43-50.

Nelson, G.C., Valin, H., Sands, R.D., Havlík, P., Ahammad, H., Deryng, D., Elliot, J., Fujimori, S., Hasegawa, T., Heyhoe, E., Kyle, P., Von Lampe, M., Lotze-Campen, H., d'Croz, D.M., van Meijl, H., van der Mensbrugghe, D., Müller, C., Popp, A., Robertson, R., Robinson, S., Schmid, E., Schmitz, C., Tabeau, A., & Willenbockel, D., 2014. Climate change effects on agriculture: economic responses to biophysical shocks. Proceedings of the National Academy of Sciences of the United States of American 111, 3274-3279. doi: 10.1073/pnas.1222465110.

Nemani, R.R., Keeling, C.D., Hashimoto, H., Jolly, W.M., Piper, S.C., Tucker, C.J., Myneni, R.B. & Running, S.W., 2003. Climate-driven increases in global terrestrial net primary production from 1982 to 1999. Science 1560-1563.

Nunes, J.P., Seixa, J., Keizer, J.J., 2013. Modeling the response of within-storm runoff and erosion dynamics to climate change in two Mediterranean watersheds: a multi-model, multi-scale approach to scenario design and analyses. Catena 102, 27–39.

O'Neal, M.R., M.A. Nearing, R.C. Vining, J. Southworth, Pfeifer., R.A., 2005. Climate change impacts on soil erosion in Midwest United States with changes in corn-soybean-wheat management. Catena 61 (2-3):165-184.

O'Gorman, P.A. & Schneider, T., 2009. The physical basis for increases in precipitation extremes in simulations of 21st-century climate change. P. Natl. Acad. Sci. USA 106, 14773-14777.

Pandey, A., Himanshu, S.K, Mishra, S.K., Singh, V.P., 2016. Physically based soil erosion and sediment yield models revisited. Catena 147, 595–620.

Pastor, A.V., Nunes, J.P., Ciampalini, R., Koopmans, M., Baartman, J., Huard, F., Calheiros, T., Le Bissonnais, Y., Keizer, J. and Raclot, D., 2019. Projecting future impacts of global change including fires on soil erosion to anticipate better land management in the forests of NW Portugal. Water 11 (12), 2617, https://doi.org/10.3390/w11122617.

Pásztor, L., Waltner, I., Centeri, C., Belényesi, M., Takács, K., 2016. Soil erosion of Hungary assessed by spatially explicit modelling. Journal of Maps. 12(1), 407–414.

Piao, S., Friedlingstein, P., Ciais, P., de Noblet-Ducoudré, N., Labat, D. & Zaehle, S., 2007. Changes in climate and land use have a larger direct impact than rising CO2 on global river runoff trends. P. Natl. Acad. Sci. USA 104, 15242-15247.

Prentice, I. C., Cramer, W., Harrison, S.P., Leemans, R., Monserud, R.A., & Soloman, A.M., 1992. Special paper: a global biome model based on plant physiology and dominance, soil properties and climate. Journal of Biogeography 19, 117-134. doi: 10.2307/2845499.

Pruski, F.F. and Nearing, M.A., 2002a. Runoff and soil loss responses to changes in precipitation: a computer simulation study. J. Soil and Water Cons. 57 (1): 7-16.

Pruski, F.F. and Nearing, M.A., 2002b. Climate-Induced Changes in Erosion during the 21st Century for Eight U.S. Locations. Water Resources Research 38 (12): art. no. 1298.

Reich, P.B., Hobbie, S.E., Lee, T.D., 2014. Plant growth enhancement by elevated CO2 eliminated by joint water and nitrogen limitation. Nature Geoscience 7, 920-924. doi: 10.1038/ngeo2284.

Rickson, R.J., 2014. Can control of soil erosion mitigate water pollution by sediments? Sci. Total Environ. 468-469, 1187-1197.

Rickson, R.J., Baggaley, N., Deeks, L.K., Graves, A., Hannam, J., Keay, C and Lilly, A., 2019. Developing a method to estimate the costs of soil erosion in highrisk Scottish catchments. Report to the Scottish Government. Available online from https://www.gov.scot/ISBN/978-1-83960-754-7.

Rogers, A., Medlyn, B.E., Dukes, J.D., Bonan, G., von Caemmerer, S., Dietze, M.C., Kattge, J., Leakey, A.D.B., Mercado, L.M., Niinemets, U., Colin Prentice, I., Serbin, S.P., Sitch, S., Way, D.A., and

Zaehle, S., 2017. A roadmap for improving the representation of photosynthesis in Earth system models. New Phytol. 213, 22–42. doi:10.1111/nph.14283.

Routschek, A., Schmidt, J., Kreienkamp, F., 2014. Impact of climate change on soil erosion? A high-resolution projection on catchment scale until 2100 in Saxony/Germany. Catena 121, 99-109.

Routschek, A., Schmidt, J., Kreienkamp, F., 2015. Climate Change Impacts on Soil Erosion: A High-Resolution Projection on Catchment Scale Until 2100. In: Engineering Geology for Society and Territory 1, 135-141.

Serpa, D., Nunes, J. P., Santos, J., Sampaio, E., Jacinto, R., Veiga, S., Lima, J.C., Moreira, M., Corte-Real, J., Keizer, J.J., Abrantes, N., 2015. Impacts of climate and land use changes on the hydrological and erosion processes of two contrasting Mediterranean catchments. Science of The Total Environment 538, 64–77.

Scholz, G., Quinton, J.N., Strauss, P., 2008. Soil erosion from sugar beet in Central Europe in response to climate change induced seasonal precipitation variations. Catena 72 (1), 91-105, doi.org/10.1016/j.catena.2007.04.005.

Skinner, R. J., & Chambers, B. J., 1996. A survey to assess the extent of soil water erosion in lowland England and Wales. Soil Use and Management 12 (4), 214–220. doi:10.1111/j.1475-2743.1996.tb00546.x.

Towers, W., Grieve, I.C., Hudson, G., Campbell, C.D., Lilly, A., Davidson, D.A., Bacon, J.R., Langan, S.J. & Hopkins, D.W., 2006. Report on the current state and threats to Scotland's soil resource. Scottish Government.

Tsara, M., Kosmas, C., Kirkby, M.J., Kosma, D., and Yassoglou, N., 2005. An evaluation of the PESERA soil erosion model and its application to a case study in Zakynthos, Greece. Soil Use and Management 21, 377–385.

UK Environment Agency, 2019. The state of the environment: soil. June 2019.

UKCP09: Hadley Centre for Climate Prediction and Research, 2017a. Observed UK climate data (1961-1990). Centre for Environmental Data Analysis. http://catalogue.ceda.ac.uk/uuid/87b3ab3b9bae47adab0c15d594d443b8

UKCP09: Hadley Centre for Climate Prediction and Research, 2017b. Probabilistic projections data of climate parameters over UK land. Centre for Environmental Data Analysis. http://catalogue.ceda.ac.uk/uuid/31cebae359e643ca9dbd1a8d0235d6fe.

Van der Sleen, P., P. Groenendijk, M. Vlam, N. P. R. Anten, A. Boom, F. Bongers, T. L. Pons, G. Terburg, and Zuidema, P.A., 2014. No growth stimulation of tropical trees by 150 years of CO_2 fertilization but water-use efficiency increased, Nat Geosci. 8, 24. doi:10.1038/ngeo2313.

Walker, M.D., Wahren, C.H., Hollister, R.D., Henry, G.H.R., Ahlquist, L.E., Alatalo, J.M., Bret-Harte, M.S., Calef, M.P., Callaghan, T.V., Carroll, A.B., Epstein, H.E., Jónsdóttir, I.S., Klein, J.A., Magnússon, B., Molau, U., Oberbauer, S.F., Rewa, S.P., Robinson, C.H., Shaver, G.R., Suding, K.N., Thompson, C.C., Tolvansen, A., Totland, O., Turner, P.L., Tweedie, C.E., Webber, P.J. & Wookey, P.A., 2006. Plant community responses to experimental warming across the tundra biome. P. Natl. Acad. Sci. 103, 1342-1346.

Watson, A., & Evans, R., 2008. Water erosion of arable fields in North-East Scotland, 1985 – 2007. Scottish Geographical Journal 123 (2), 107–121. doi:10.1080/14702540701474287.

Whiting, P.J., Bonniwell, E.C. & Matisoff, G., 2001. Depth and areal extent of sheet and rill 613 erosion based on radionuclides in soils and suspended sediment. Geology 29, 1131-1134. 614. https://doi.org/10.1130/0091-7613(2001)029%3C1131:DAAEOS%3E2.0.CO;2.

Xiong, M., Sun, R., & Chen, L., 2019. A global comparison of soil erosion associated with land use and climate type. Geoderma 343, 31–39. doi:10.1016/j.geoderma.2019.02.013.

Zhang, Y.-G., M. Hernandez, E. Anson, M.A. Nearing, H. Wei, J.J. Stone, Heilman, P., 2012. Modeling climate change effects on runoff and soil erosion in southeastern Arizona rangelands and implications for mitigation with rangeland conservation practices. J. Soil and Water Conservation 67 (5), 390-405.

Zhang, X.C. & Nearing, M.A., 2005. Impact of Climate Change on Soil Erosion, Runoff, and Wheat Productivity in Central Oklahoma. Catena 61 (2-3), 185-195.

Zuazo, V.H.D., & Pleguezuelo, C.R.R., 2008. Soil-erosion and runoff prevention by plant covers. A review. Agronomy for Sustainable Development 28 (1), 65–86. doi:10.1051/agro:2007062.

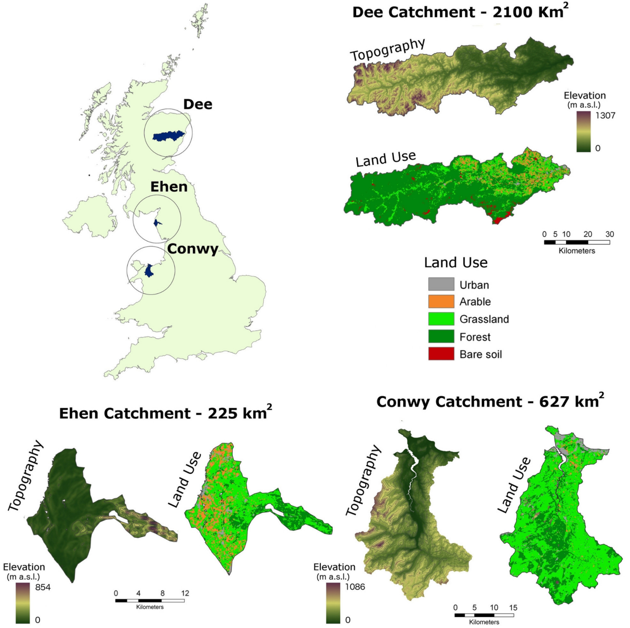

Dee
Ehen
Conwy
Dee Catchment - 2100 Km²
Topography
Elevation
(m a.s.l.)
1307
0
Land Use
0 5 10 20 30
Kilometers
Land Use
Urban
Arable
Grassland
Forest
Bare soil
Ehen Catchment - 225 km²
Topography
Land Use
Elevation
(m a.s.l.)
854
0
0 4 8 12
Kilometers
Conwy Catchment - 627 km²
Topography
Land Use
Elevation
(m a.s.l.)
1086
0
0 5 10 15
Kilometers

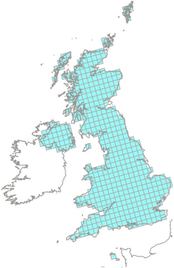

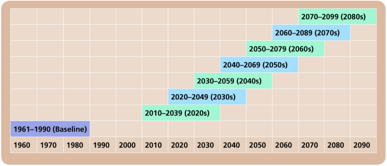
2070–2099 (2080s)
2060–2089 (2070s)
2050–2079 (2060s)
2040–2069 (2050s)
2030–2059 (2040s)
2020–2049 (2030s)
2010–2039 (2020s)
1961–1990 (Baseline)
1960
1970
1980
1990
2000
2010
2020
2030
2040
2050
2060
2070
2080
2090

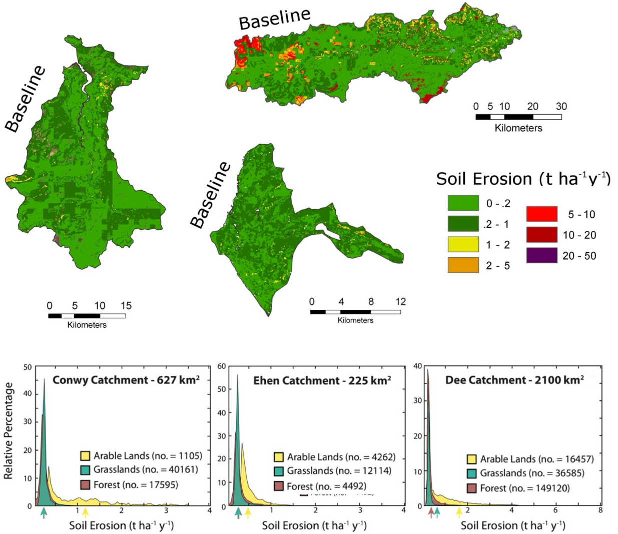
Baseline
Baseline
Baseline
0 5 10 20 30
Kilometers
Soil Erosion (t ha⁻¹y⁻¹)
0 - .2
.2 - 1
1 - 2
2 - 5
5 - 10
10 - 20
20 - 50
0 5 10 15
Kilometers
0 4 8 12
Kilometers
Conwy Catchment - 627 km²
Arable Lands (no. = 1105)
Grasslands (no. = 40161)
Forest (no. = 17595)
Ehen Catchment - 225 km²
Arable Lands (no. = 4262)
Grasslands (no. = 12114)
Forest (no. = 4492)
Dee Catchment - 2100 km²
Arable Lands (no. = 16457)
Grasslands (no. = 36585)
Forest (no. = 149120)
Relative Percentage
Soil Erosion (t ha⁻¹ y⁻¹)
Soil Erosion (t ha⁻¹ y⁻¹)
Soil Erosion (t ha⁻¹ y⁻¹)

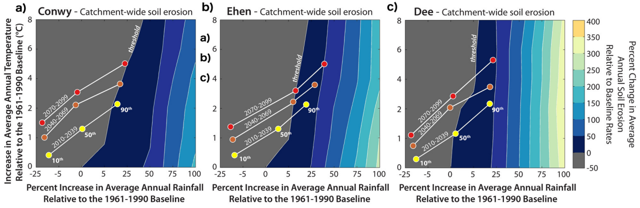
a) Conwy - Catchment-wide soil erosion
b) Ehen - Catchment-wide soil erosion
c) Dee - Catchment-wide soil erosion
Increase in Average Annual Temperature Relative to the 1961-1990 Baseline (°C)
Percent Increase in Average Annual Rainfall Relative to the 1961-1990 Baseline
threshold
2070-2099
2040-2069
2010-2039
10th
50th
90th
a)
b)
c)
Percent Change in Average Annual Soil Erosion Relative to Baseline Rates
400
350
300
250
200
150
100
50
0
-50

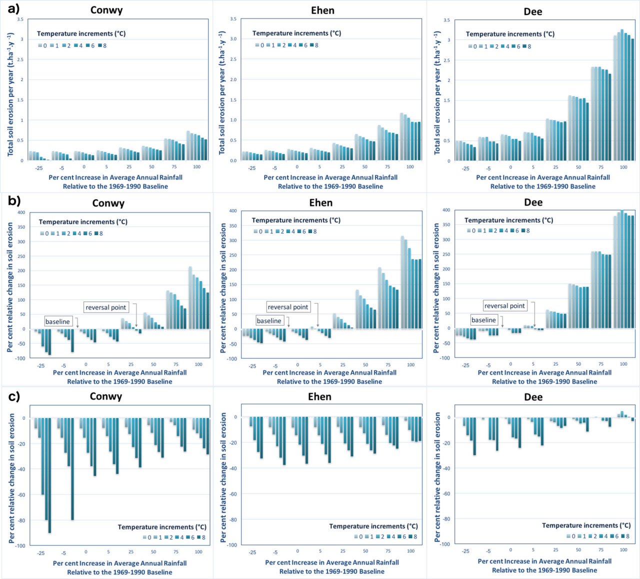

a)
Conwy
Ehen
Dee
Total soil erosion per year (t.ha-1.y-1)
Temperature increments (°C)
0 1 2 4 6 8
Per cent Increase in Average Annual Rainfall
Relative to the 1969-1990 Baseline
-25 -5 0 5 25 50 75 100
b)
Conwy
Ehen
Dee
Per cent relative change in soil erosion
baseline
reversal point
c)
Conwy
Ehen
Dee

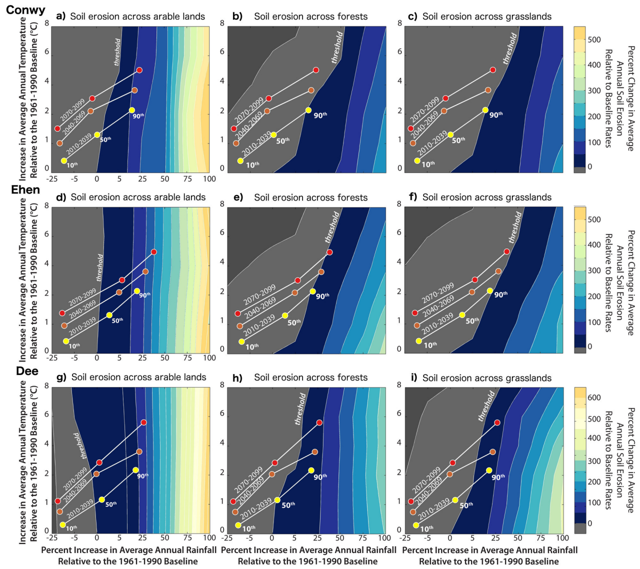

Conwy
a) Soil erosion across arable lands
b) Soil erosion across forests
c) Soil erosion across grasslands
Ehen
d) Soil erosion across arable lands
e) Soil erosion across forests
f) Soil erosion across grasslands
Dee
g) Soil erosion across arable lands
h) Soil erosion across forests
i) Soil erosion across grasslands
threshold
2070-2099
2040-2069
2010-2039
10th
50th
90th
Increase in Average Annual Temperature Relative to the 1961-1990 Baseline (°C)
Percent Increase in Average Annual Rainfall Relative to the 1961-1990 Baseline
Percent Change in Average Annual Soil Erosion Relative to Baseline Rates
-25
-5
0
5
25
50
75
100
0
2
4
6
8
100
200
300
400
500
600

Table 1. Type and land use percentage in the three catchments.

Land use	Conwy	Ehen	Dee
Artificial	3.2	4.5	1.0
Arable land	1.8	0.7	7.9
Forage/Fallow	0.0	18.7	0.0
Grassland	64.0	55.0	17.5
Forest	28.0	20.4	71.2
Bare land	1.7	0.7	0.3
Water surface	1.2	0.0	2.1

Table 2. Planting calendar. Dark green cells denote planting months, with the percentage of vegetation cover by each agricultural type provided in subsequent months (light green). Yellow cells denote the harvesting month, with vegetation cover equalling zero afterwards.

Conwy	**planting**	**Month 1**	**Month 2**	**Month 3**	**Month 4**	**Month 5**	**Month 6**	**Month 7**	**Month 8**	**Month 9**	**Month 10**	**Month 11**	**Month 12**
Vegetables	March	-	April	May	June	July	August						
/Flowers		-	18	64	98	91	45						

Ehen	**planting**	**Month 1**	**Month 2**	**Month 3**	**Month 4**	**Month 5**	**Month 6**	**Month 7**	**Month 8**	**Month 9**	**Month 10**	**Month 11**	**Month 12**
Pulses	February	March	April	May	June								
		19	66	98	72								
Rootcrops	February	March	April	May	June	July	August						
		11	68	99	94	86	36						
Vegetables	March	-	April	May	June	July	August						
/Flowers		-	18	64	98	91	45						
Forage	August	March	April					September	October	November	December	January	February
(Winter)		70	54					10	67	69	72	77	81
Forage	February	March	April	May	June	July	August	September	October				
(Summer)		10	67	69	72	77	81	70	54				
	Planting	**Month 7**	**Month 8**	**Month 9**	**Month 10**	**Month 11**	**Month 12**	**Month 1**	**Month 2**	**Month 3**	**Month 4**	**Month 5**	**Month 6**
Oilseeds	September	March	April	May	June	July	August	September	October	November	December	January	February
		84	86	87	87	90	45	18(13)	64	72	77	79	80

Dee	**Planting**	**Month 1**	**Month 2**	**Month 3**	**Month 4**	**Month 5**	**Month 6**	**Month 7**	**Month 8**	**Month 9**	**Month 10**	**Month 11**	**Month 12**
Rootcrops	February	March	April	May	June	July	August						
		11	68	99	94	86	36						

Vegetables	March	-	April	May	June	July	August						
/Flowers		-	18	64	98	91	45						

Table 3. Climatic variables and soil erosion averages for the three catchments. Rainfall (mm), temperature (°C), and resulting soil erosion (t $ha^{-1}y^{-1}$) for baseline (upper table), and for 2010/39, 2040/69 and 2070/99 periods at p10, p50 and p90 prediction level probability (t $ha^{-1}y^{-1}$ and percent variation) (lower tables).

		Rainfall (mm)	Temp. (°C)	Erosion catchment (t ha^{-1} y^{-1})	Erosion Forest (t ha^{-1} y^{-1})	Erosion Grassland (t ha^{-1} y^{-1})	Erosion Arable (t ha^{-1} y^{-1})
Baseline	**Conwy**	95.4	8.1	0.24	0.20	0.22	1.17
	Ehen	71.9	8.2	0.28	0.25	0.23	0.48
	Dee	113.9	5.3	0.65	0.62	0.32	1.62
	Average	93.73	7.17	0.39	0.36	0.26	1.09

		2010/39				2040/69				2070/99			
		Rainfall (mm)	Temp. (ºC)	Erosion (t $ha^{-1} y^{-1}$)	Erosion Var. %	Rainfall (mm)	Temp. (ºC)	Erosion (t $ha^{-1} y^{-1}$)	Erosion Var. %	Rainfall (mm)	Temp. (ºC)	Erosion (t $ha^{-1} y^{-1}$)	Erosion Var. %
p10	Conwy	82.3	8.5	0.19	-20.8	78.6	9.1	0.17	-29.2	76.6	9.6	0.16	-33.3
	Ehen	63.0	8.6	0.23	-17.9	61.8	9.1	0.22	-21.4	60.4	9.5	0.20	-28.6
	Dee	97.7	5.6	0.48	-26.2	93.1	6.0	0.44	-32.9	91.5	6.4	0.42	-35.8
p50	Conwy	95.5	9.4	0.21	-12.5	94.2	10.3	0.19	-20.8	94.5	11.2	0.18	-25.0
	Ehen	73.8	9.5	0.27	-3.6	75.4	10.3	0.28	0.0	77.0	11.1	0.28	0.0
	Dee	115.1	6.4	0.66	1.5	113.8	7.3	0.57	-12.3	114.5	8.1	0.56	-14.5
p90	Conwy	111.1	10.4	0.25	4.2	113.3	11.7	0.23	-4.2	117.4	13.1	0.23	-4.2
	Ehen	86.6	10.4	0.34	21.4	92.6	11.7	0.39	39.3	99.2	13.1	0.45	60.7
	Dee	135.7	7.5	0.95	46.2	139.4	8.9	0.85	31.1	144.3	8.9	0.90	38.4

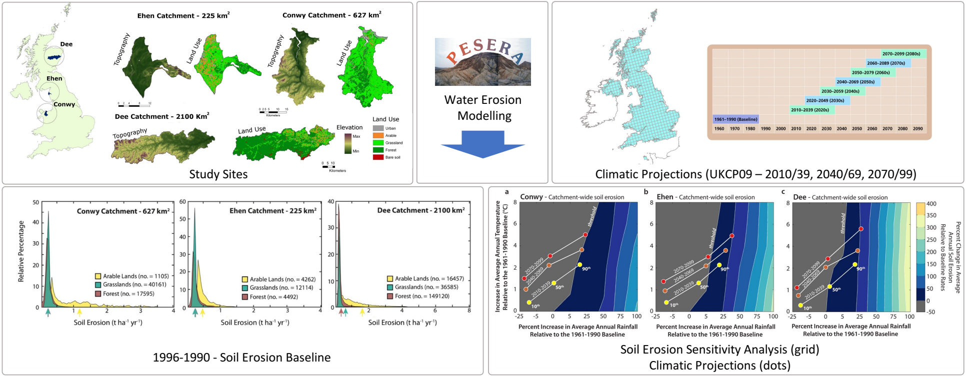
Ehen Catchment - 225 km²
Conwy Catchment - 627 km²
Dee Catchment - 2100 Km²
Dee
Ehen
Conwy
Topography
Land Use
Elevation
Max
Min
Land Use
Urban
Arable
Grassland
Forest
Bare soil
Kilometers
Study Sites
PESERA
Water Erosion Modelling
2070–2099 (2080s)
2060–2089 (2070s)
2050–2079 (2060s)
2040–2069 (2050s)
2030–2059 (2040s)
2020–2049 (2030s)
2010–2039 (2020s)
1961–1990 (Baseline)
1960 1970 1980 1990 2000 2010 2020 2030 2040 2050 2060 2070 2080 2090
Climatic Projections (UKCP09 – 2010/39, 2040/69, 2070/99)
Relative Percentage
Conwy Catchment - 627 km²
Arable Lands (no. = 1105)
Grasslands (no. = 40161)
Forest (no. = 17595)
Ehen Catchment - 225 km²
Arable Lands (no. = 4262)
Grasslands (no. = 12114)
Forest (no. = 4492)
Dee Catchment - 2100 km²
Arable Lands (no. = 16457)
Grasslands (no. = 36585)
Forest (no. = 149120)
Soil Erosion (t ha⁻¹ yr⁻¹)
1996-1990 - Soil Erosion Baseline
a Conwy - Catchment-wide soil erosion
b Ehen - Catchment-wide soil erosion
c Dee - Catchment-wide soil erosion
Increase in Average Annual Temperature Relative to the 1961-1990 Baseline (°C)
threshold
2070-2099
2040-2069
2010-2039
10th
50th
90th
Percent Increase in Average Annual Rainfall Relative to the 1961-1990 Baseline
Percent Change in Average Annual Soil Erosion Relative to Baseline Rates
Soil Erosion Sensitivity Analysis (grid)
Climatic Projections (dots)